Feasibility of conductivity imaging based on slice selection and readout gradient induced eddy-currents

Omer Faruk Oran[1], Necip Gurler[1], and Yusuf Ziya Ider[1]
[1]*Electrical and Electronics Engineering, Bilkent University, Ankara, Turkey*

Introduction: Electrical conductivity of human tissues differs by type and pathological state and also it shows frequency dependence. Several methods have been developed for imaging electrical conductivity at high (i.e. Larmor frequency) or low (up to 1 kHz) frequencies. Recently it has been proposed to utilize eddy-currents induced during the rise-time of the readout gradient for imaging conductivity at low frequencies [1, 2]. However, conductivity reconstruction using experimental data has not been presented yet in any study. In this study, for current MRI technology, we investigate the feasibility of conductivity imaging using slice-selection or readout gradient induced eddy-currents.

Theory: Time-varying gradient fields in MRI cause eddy currents to be induced on the conducting structures of the MRI scanner such as RF coils, RF shields and components of the main magnet and, if conductive, in the imaging subject. The gradient induced eddy-currents cause additional magnetic fields which create undesired effects such as ghosting, geometric distortion [3]. It is found that the induced currents on the conducting structures decay with multiple exponential decay constants [3]. Therefore each conducting structure can be approximately modeled using separate inductive-resistive (LR) circuits. Mutual inductances between conducting structures and gradient coils along with the parameters L (self-inductance) and R determine the induced current in each LR circuit and the additional magnetic field is proportional to this induced current. The mutual and self-inductances depend on the geometry and position of the conducting structures and R depends on the material type. The empirical findings suggest that the eddy-current decay time-constants (corresponds to L/R in the model) for conducting structures are in the order of from tens of milliseconds up to 1 second. Considering the fact that objects to be imaged have substantially higher R than other conducting structures (compare human body to copper), eddy currents induced in the imaging subject decays faster to the extent that they may be assumed to be vanish instantly once the time-derivative of the gradient field becomes zero.

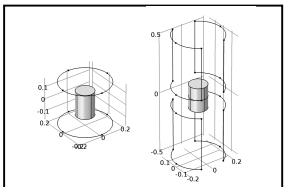

Fig 1. Wire-model of the coils. (a) Maxwell (b) Saddle Golay

Methods: a) Analytical Model: In order to verify the simulation process and to analyze eddy-current induced by slice-selection gradient, a simple analytical model is developed. In this model, a z-oriented cylindrical object which is centered at the z-axis and which has radius of 7.2 cm, height of 22 cm, and conductivity of 1 S/m is assumed. During the rise-time of slice selection gradient field, B-field at any slice is given by $\mathbf{B}(t) = \hat{a}_z Kzt$ where K is the slew-rate of the gradient field. The induced eddy-current on a circle of radius r which is located on a constant-z plane is found from the integral form of Faraday's Law as $\oint \mathbf{E} \cdot \mathrm{dl} = -\iint \frac{\partial \mathbf{B}}{\partial t} \cdot \mathrm{dA} \rightarrow \frac{J}{\sigma} 2\pi r = -Kz\pi r^2 \rightarrow J = -\frac{\sigma Kzr}{2}$. Once analytical expression for J is found, Biot-savart law is used for calculation of the secondary magnetic field due to eddy-currents.

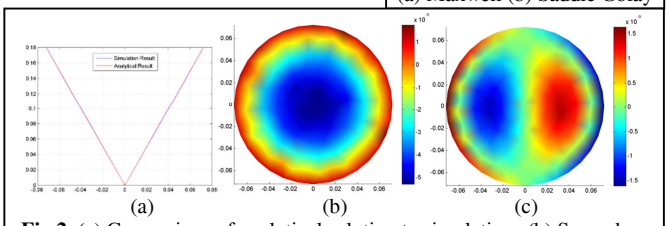

(a) (b) (c)

Fig 2. (a) Comparison of analytical solution to simulations (b) Secondary B-field due to eddy-currents induced by z-gradient (c) by x-gradient

b) Simulation Methods: For the simulations Comsol Multiphysics FEM software package is used for the time-domain solution of the equation $\sigma \frac{\partial \mathbf{A}}{\partial t} + \nabla \times \mathbf{B} = \mathbf{J}_e$ where σ is the conductivity, $\mathbf{A}$ is the vector potential, $\mathbf{B}$ is the magnetic field which consists of primary (due to gradient coil) and secondary (due to eddy-current) magnetic fields and $\mathbf{J}_e$ is the external (source) current density which is defined only on the gradient coil. $\mathbf{J}_e$ is given as a ramp function in time and by adjusting the slope of this function, desired slew-rate of the gradient field is obtained. In deriving this equation, quasistatic assumption is used ($\sigma \gg \omega\epsilon$) and the gauge for vector potential is such that the electric potential vanishes. In this case, the induced eddy-current is simply $J = \sigma \frac{\partial \mathbf{A}}{\partial t}$ and again Biot-savart law is used for calculation of the secondary magnetic field due to eddy-currents. For generating z-gradient field, a Maxwell coil is obtained using wire-model and for generating x-gradient field a Saddle-Golay coil is obtained using wire-model. Wire-models for both coils along with the cylindrical object used in analytical model are shown in Fig 1.(a) and (b).

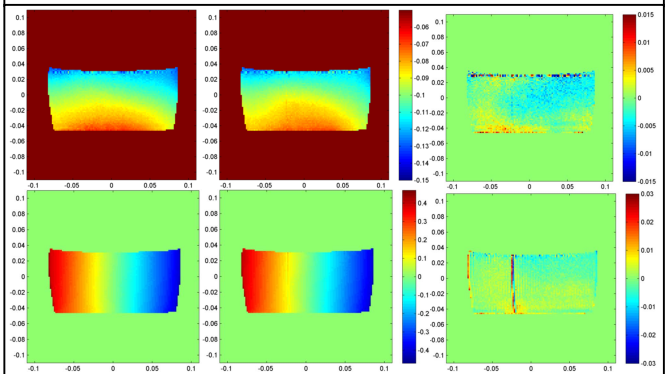

Fig 3. Eddy current phase for first and second exp. (left-middle), their diff. (right).Top Row: Slice-Selection Gradient, Bottom Row: Readout Gradient

c) Experimental Methods: For the experiments a rectangular container of dimensions 15.6x24 cm is filled with agar (20 gr/l agar, 1 gr/l CuSO4, 6 gr/l NaCl) of height 8.19 cm. The eddy-current phase for slice-selection gradient is measured by consecutively applying two spin-echo sequences with reverse slice-selection gradient polarity and the eddy-current phase for read-out gradient is similarly measured by applying two spin-echo sequences with reverse readout gradient polarity. The MRI image phases of different gradient polarities are then subtracted to obtain the phase due to eddy currents. In order to eliminate the phase of eddy-currents induced on conducting structures of MR scanner, we conduct two experiments and in the second experiment, the agar phantom, is divided into two compartments by a thin insulating plate.

Results: For the cylindrical object described in the analytical model, the induced eddy-current distribution due to z-gradient is very similar to the distribution obtained with analytical model as shown in Fig. 2 (a). Therefore our simulation process is verified. In Fig 2(b) the secondary B-field is given. For this simulation case, slew-rate is taken to be 100 T/m/sec. If the final value of the gradient is taken to be 10 mT/m then this B-field distribution can only accumulate $4x10^{-5}$ rad which is far from being measurable. In Fig 2(c) secondary B-field is given for the same phantom when readout gradient is applied. The accumulated phase is again around $4x10^{-5}$ rad and thus again not measurable. Fig 3. summarizes the experimental results. As expected from the simulations performed, dividing the agar phantom into two compartments does not change measured phase and thus we conclude that the measured phase is coming only from the eddy-currents induced on the conducting structures.

Discussion and Conclusion: By simulations and experiments we conclude that eddy-currents induced in the imaging object has a very low magnitude and thus does not generate measurable amount of secondary B-field. Therefore conductivity imaging using this secondary B-field seems to be unfeasible unless extremely high (impractical for present day MRI technology) gradients are used.

Acknowledgements: Experimental data are acquired using the facilities of UMRAM, Bilkent University, Ankara

References: [1] van Lier et al, *ISMRM 2012*:3467 [2] Oran et al ISMRM 2013:5271 [3] Bernstein, "Handbook of MRI pulse sequences", 2004